




The Cytotoxicity of Epsilon Toxin from *Clostridium perfringens* on Lymphocytes Is Mediated by MAL Protein Expression

Marta Blanch,^{a,b,c} Jonatan Dorca-Arévalo,^{a,b,c} Anna Not,^a Mercè Cases,^{a,b,c} Inmaculada Gómez de Aranda,^{a,c} Antonio Martínez-Yélamos,^{b,d} Sergio Martínez-Yélamos,^{b,d} Carles Solsona,^{a,b,c}  Juan Blasi^{a,b,c}

^aLaboratory of Cellular and Molecular Neurobiology, Department of Pathology and Experimental Therapeutics, Campus of Bellvitge, University of Barcelona, Hospitalet de Llobregat, Barcelona, Spain

^bBiomedical Research Institute of Bellvitge (IDIBELL), Hospitalet de Llobregat, Barcelona, Spain

^cInstitute of Neurosciences, University of Barcelona, Barcelona, Spain

^dNeurology Department, Bellvitge University Hospital, Hospitalet de Llobregat, Barcelona, Spain

ABSTRACT Epsilon toxin (Etx) from *Clostridium perfringens* is a pore-forming protein that crosses the blood-brain barrier, binds to myelin, and, hence, has been suggested to be a putative agent for the onset of multiple sclerosis, a demyelinating neuroinflammatory disease. Recently, myelin and lymphocyte (MAL) protein has been identified to be a key protein in the cytotoxic effect of Etx; however, the association of Etx with the immune system remains a central question. Here, we show that Etx selectively recognizes and kills only human cell lines expressing MAL protein through a direct Etx-MAL protein interaction. Experiments on lymphocytic cell lines revealed that MAL protein-expressing T cells, but not B cells, are sensitive to Etx and reveal that the toxin may be used as a molecular tool to distinguish subpopulations of lymphocytes. The overall results open the door to investigation of the role of Etx and *Clostridium perfringens* on inflammatory and autoimmune diseases like multiple sclerosis.

KEYWORDS *Clostridium perfringens*, multiple sclerosis, myelin and lymphocyte protein, T cell, epsilon toxin, pore-forming toxins

Epsilon toxin (Etx) from *Clostridium perfringens* toxinotypes B and D is the most powerful toxin after botulinum and tetanus toxins, mainly affecting ruminants and causing important economic losses (1). The toxin is produced by the bacteria present in the guts of young animals, leading to fatal enterotoxemia in sheep, goats, and cattle (2, 3). It is synthesized as a nontoxic protein precursor, epsilon prototoxin (pEtx), which is activated upon proteolytic cleavage at the N- and C-terminal regions (4).

In addition to its effect on livestock, Etx has lethal activity when injected into experimental animal models, basically, rodents. Etx bypasses the transit through the digestive system and causes a generalized edema, neurological disorders, and, finally, the death of the animal, with the lethal dose in mice (one of the animal models most used for Etx studies) being about 100 ng/kg of body weight (5). At the cellular level, Etx is a member of the aerolysin-like β pore-forming toxin family (6). Etx forms pores in lipid planar bilayers and therefore in the plasma membrane of sensitive cells after its specific binding and further oligomerization, producing cell permeability, ionic diffusion, ATP depletion, and cell death (7, 8). The toxin also has the capacity to cross the blood-brain barrier (BBB) and bind to cerebral myelin (9, 10). Moreover, *in vitro* experiments using primary cell cultures and brain explants have demonstrated the demyelination capacity of Etx and, eventually, its cytotoxic effect on oligodendrocytes (10, 11), the myelin-forming cells in the central nervous system. These and other evidences have been used as arguments to suggest that Etx is a putative agent for the onset of multiple sclerosis (MS), a neuroinflammatory disease with a demyelinating component (12).

Received 19 February 2018 Returned for modification 1 April 2018 Accepted 29 June 2018

Accepted manuscript posted online 9 July 2018

Citation Blanch M, Dorca-Arévalo J, Not A, Cases M, Gómez de Aranda I, Martínez-Yélamos A, Martínez-Yélamos S, Solsona C, Blasi J. 2018. The cytotoxicity of epsilon toxin from *Clostridium perfringens* on lymphocytes is mediated by MAL protein expression. *Mol Cell Biol* 38:e00086-18. <https://doi.org/10.1128/MCB.00086-18>.

Copyright © 2018 American Society for Microbiology. All Rights Reserved.

Address correspondence to Juan Blasi, blasi@ub.edu.

In addition to the effect of Etx on oligodendrocytes, a few cell lines have been defined to be sensitive to Etx and identified as potential targets of its cytotoxic activity. Among them, the most sensitive cell line is the Madin-Darby canine kidney (MDCK) cell line, a renal epithelial distal tubule cell line from canine origin which has been widely used to study the cellular and molecular mechanism of Etx cytotoxicity (8). This characteristic of the renal cell line correlates with the observed *in vivo* cytotoxic effect of Etx on renal distal tubular cells in Etx-injected mice (13, 14). Other cell lines that are sensitive to Etx but in which it has a variable cytotoxic effect, depending on the cell model, include the mouse kidney cell line mpkCCD_{c14} (15), the Caucasian renal leiomyoblastoma (G-402) human cell line (16), primary cultures of human renal tubular epithelial cells (HRTEC) (17), and the human renal adenocarcinoma cell line ACHN (18), among others.

It is assumed that the specific action of Etx on sensitive cells relies on the presence of an Etx receptor so that it may selectively bind the cell surface before the formation of the oligomer. In spite of the proposed role of membrane lipids in the recognition of cell targets by Etx or the affinity of Etx to cell targets (19–21), a set of proteins which can account for the full and highly sensitive effect of the toxin has been explored as potential receptors for Etx. Among them, the most promising candidates are the hepatitis A virus cellular receptor 1 (HAVCR1) (18) and the myelin and lymphocyte (MAL) protein (22). While complete functional evidence for HAVCR1 as an Etx receptor mediating its cytotoxic activity is elusive (23), the transfection of MAL protein confers sensitivity to otherwise unresponsive cell lines (22). In addition, mice in which MAL protein is knocked out survive after intraperitoneal injection of a lethal dose of Etx (22). Accordingly, myelin and lymphocyte (MAL) protein has been defined to be a key protein in the cytotoxic effect of Etx, either as a putative receptor or as an effector protein (23).

MAL protein is a tetraspanning membrane protein of 17 kDa initially identified to be a marker of human T cell maturation (24). This protein is also present in myelinating oligodendrocytes, myelin, and some epithelial cells (i.e., urothelial and renal tubules), where it has been involved in membrane traffic, especially for the apical transport of membrane and secretory proteins and lipid raft cycling (25, 26). The presence of MAL protein in myelin structures and myelinating oligodendrocytes would explain the specific binding of Etx to myelin (9) and the demyelinating effect of the toxin (10, 11). The presence of MAL protein in lymphocytes has been mainly linked to the maturation of T cells (24), intracellular membrane traffic (27), or exosome secretion (28). However, the possible effect of Etx on MAL protein-expressing lymphocyte-derived cells is not known.

In the present paper, we further explore by several methods whether the cytotoxic ability of Etx from *Clostridium perfringens* is exclusively dependent on the expression of MAL protein. Moreover, evidence of a direct interaction of MAL protein with Etx is provided by means of immunoprecipitation assays. These results led us explore the sensitivity to Etx of cell lines from lymphocytic origin which naturally express or do not express MAL protein, and we demonstrate that this protein is sufficient for Etx cytotoxic activity. The study of cell types that naturally express MAL protein would give a new light on the Etx action mechanism and its relationship with immune system-related disorders.

RESULTS

MAL protein is required for Etx binding. To characterize the MAL protein-dependent cytotoxic effect of Etx, three cell lines which do not express MAL protein (tsA201, RT4-D6P2T, and HeLa) were stably transfected for the expression of human MAL protein (hMAL) fused to green fluorescent protein (GFP) (hMAL-GFP). Mock-transfected (GFP) cells were used as controls.

Transfected cells were positively selected with 0.5 mg/ml G418 (Geneticin) before cell sorting was performed, and the most positive cells expressing hMAL-GFP were collected, maintained, and used for further experiments. The effectiveness of hMAL-GFP

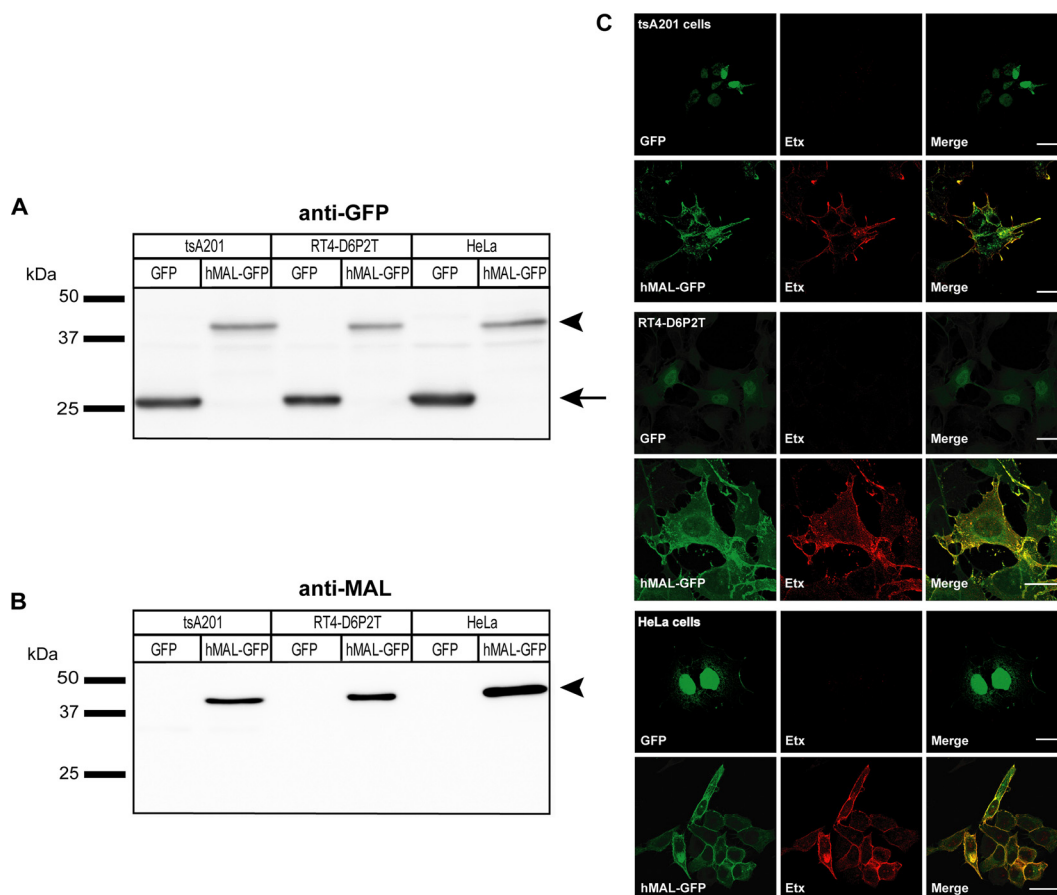


FIG 1 Specific binding of Etx to the plasma membrane of hMAL-GFP-expressing cell lines. (A, B) Western blot analysis of stable tsA201, RT4-D6P2T, and HeLa cell lines expressing either GFP or hMAL-GFP. (A) Expression of GFP (27 kDa, arrow) and hMAL-GFP (44 kDa, arrowhead) was detected with anti-GFP. (B) Expression of hMAL-GFP (44 kDa, arrowhead) was detected with anti-MAL-E1. (C) Confocal microscopy images from tsA201, RT4-D6P2T, and HeLa cells expressing hMAL-GFP or GFP and incubated with 100 nM labeled Etx-633 for 1 h (see Materials and Methods). The hMAL-GFP protein (green) exquisitely colocalized with Etx-633 (red) on the plasma membrane, while the Etx-633 signal was not detected in control cells, which express only GFP. Bars, 25 μ m.

expression was monitored by Western blot analysis using anti-GFP and anti-MAL-E1 antibodies (Fig. 1A and B, respectively).

Confocal microscopy images revealed the expression of hMAL-GFP mostly localized in the cell plasma membrane, while GFP was localized in the cytosol and nuclei in mock-transfected cells (Fig. 1C).

Etx labeled with DyLight 633 (Etx-633) was used to verify the binding of Etx to positive hMAL-GFP-expressing cells. As expected, the toxin was bound to the cell lines expressing hMAL-GFP but not to the GFP-expressing control cell lines. Most of the Etx labeling was localized in the periphery of the cells, matching the distribution of hMAL-GFP (Fig. 1C).

Etx produces cytotoxicity in hMAL-expressing cells. The cytotoxic effect of Etx is based on the selective binding to the target cell, the oligomerization of the protein, and the subsequent pore formation that permeabilizes the cell plasma membrane, allowing the diffusion of ions and other elements up to 2.3 kDa (29, 30).

Taking advantage of the pore-forming capacity of Etx, the release of ATP from the cytosol or internal cell stores was measured using the luciferin-luciferase method on hMAL-GFP-expressing cells, on MDCK cells, used as positive controls, and on GFP-transfected cells, used as negative controls.

ATP release from MDCK cells was Etx dose and time dependent (Fig. 2A). All content of ATP was released between 30 min (100 nM Etx) and 40 min (12.5 nM), depending on the Etx dose.

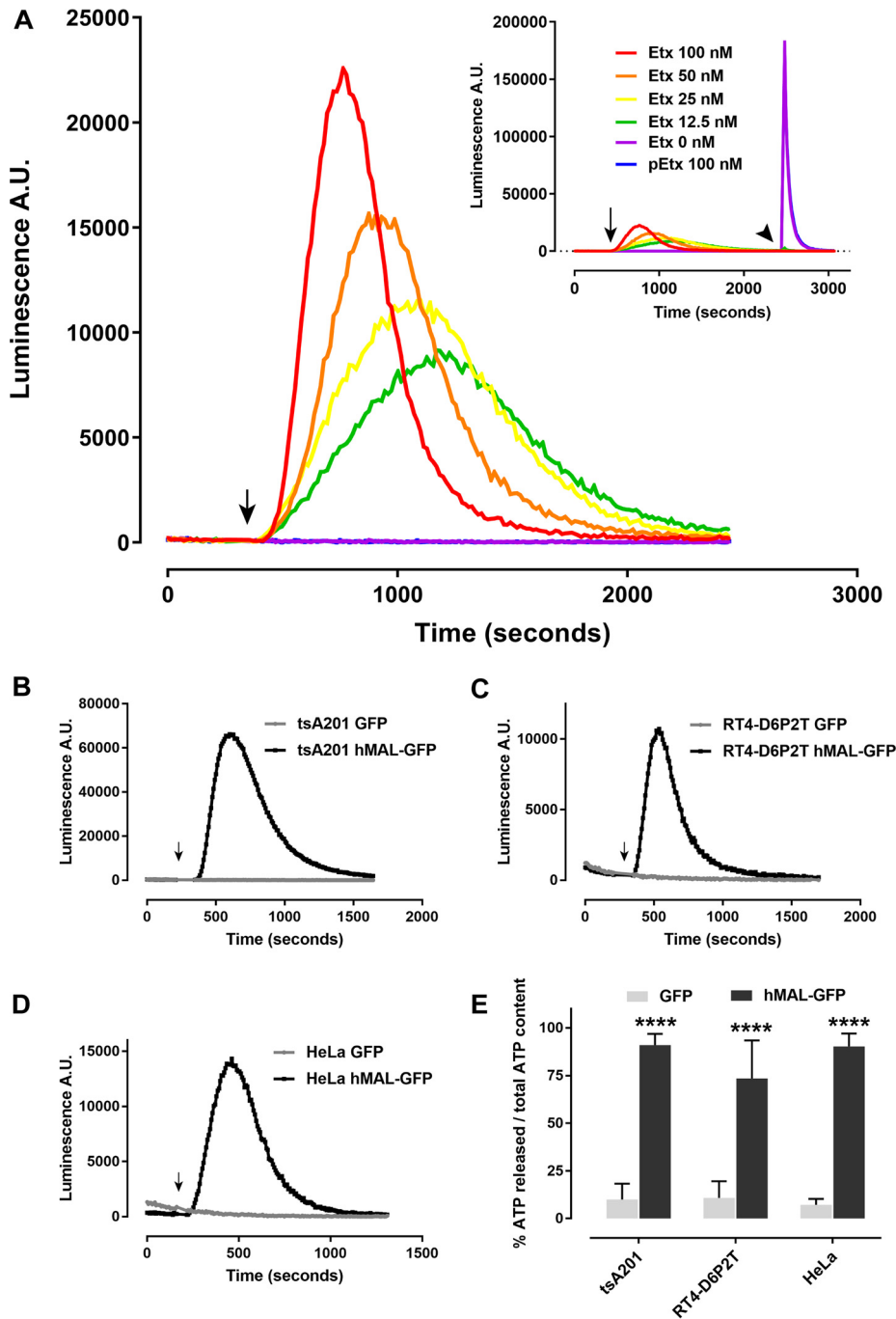


FIG 2 Etx-dependent ATP release from MDCK cells and from the tsA201, RT4-D6P2T, and HeLa cell lines expressing hMAL-GFP. (A) ATP release from MDCK cells. MDCK cells were incubated with different concentrations of Etx (arrow, time of Etx addition); the release of ATP was monitored continuously as light emission (A.U., arbitrary units of luminescence). Etx produced the release of ATP from treated cells at all concentrations used, although the kinetics was accelerated at higher Etx concentrations. No ATP release was recorded when MDCK cells were incubated with pEtx at a concentration equivalent to the maximum concentration of Etx used or when Etx was not added to the incubation medium (0 nM). (Inset) At the end of the experiment, Triton X-100 was added (0.2% final concentration, arrowhead) to release the remaining ATP. The release of the ATP content was clearly observed in control cells (0 nM) and when cells were incubated with pEtx. (B to D) ATP release from hMAL-GFP- or GFP-expressing cells: tsA201 cells (B), RT4-D6P2T cells (C), and HeLa cells (D). Etx (100 nM) was added (arrow) to transfected cell lines expressing hMAL-GFP or GFP alone, and ATP release was monitored as described for panel A. ATP was released only from cells expressing hMAL-GFP and not from cells expressing GFP alone. Triton X-100 (0.2% final concentration) was added at the end of the experiment to estimate the total content of ATP in the cells (not shown). (E) The bar chart shows the percentage of the Etx-induced release of ATP with respect to the total ATP content under each condition (B to D). Each condition was run in triplicate and in three independent experiments (****, $P < 0.0001$).

The concentrations of Etx used (from 12.5 to 100 nM) were rather high, considering the sensitivity of the MDCK cell line to Etx, but this approach was very convenient because it allowed the measurement in real time of Etx-dependent ATP release in a limited time. At the end of the experiment, all ATP was virtually released by Etx and no residual ATP could be measured after cell permeabilization with Triton X-100. However, Triton X-100 released all ATP content in the case of GFP-expressing cells or when pEtx was used instead of fully active Etx. These results suggest that at all concentrations used, the MDCK cells were already dead at the end of the experiment in spite of the Etx concentration used (Fig. 2A).

As expected, hMAL-GFP-transfected cells released ATP in the presence of Etx (Fig. 2B to D); however, no ATP was released from GFP-transfected cells or from those cells incubated in the presence of pEtx, even at the highest concentration used. These results support pore formation by Etx (anionic or nonspecific) in hMAL-expressing cells, although the possibility of the rupture of the plasma membrane by some other mechanism (i.e., necrosis) cannot be discarded.

The 3-(4,5-dimethylthiazol-2-yl)-5-(3-carboxymethoxyphenyl)-2-(4-sulfophenyl)-2H-tetrazolium (MTS) colorimetric assay was used in cytotoxicity assays to determine cell viability (see Materials and Methods). The MTS assays revealed that Etx and Etx-633 showed a similar degree of cytotoxicity to hMAL-GFP-expressing cells, with no effect on GFP-expressing control cells. The nonactive forms of the toxin, pEtx or pEtx-633, showed no toxic effects (not shown). The cytotoxic effect of Etx on hMAL-GFP-transfected cell lines was similar to that observed in MDCK cells (Fig. 3), although this effect was not complete in all transfected cell lines (no 100% cell death), suggesting levels of hMAL-GFP expression different from those in the well-established and sensitive MDCK cell line. The cytotoxicity of Etx on hMAL-GFP-transfected cell lines was dose dependent, with a maximum effect at about 25 nM. The 50% cytotoxic concentration (CT_{50}) was calculated with a 95% confidence interval (CI; lower-upper values). In the case of tsA201 cells expressing hMAL-GFP, the CT_{50} was 1.26 nM (95% CI, 0.69 to 2.27 nM), in RT4-D6P2T cells expressing hMAL-GFP, the CT_{50} was 2.88 nM (95% CI, 2.36 to 3.50 nM), and finally, in HeLa cells expressing hMAL-GFP, the CT_{50} was 3.36 nM (95% CI, 2.63 to 4.29 nM). All of these values were not far from the CT_{50} calculated for MDCK cells, 0.64 nM (95% CI, 0.52 to 0.78 nM).

Direct hMAL-Etx interaction. Considering that transfection of hMAL-GFP in a nonsensitive cell line was able to transform these cells into an Etx-sensitive state (as seen in the MTS assays and ATP release experiments), it was essential to search for a possible Etx-MAL protein interaction.

In order to check for a possible Etx-MAL protein interaction, coimmunoprecipitation (co-IP) assays were performed with the hMAL-GFP-expressing HeLa stable cell line. Cells were grown in four confluent culture dishes 10 cm in diameter; the cells in two of the dishes were exposed to 100 nM Etx for 30 min, the cells in one dish were exposed to 100 nM pEtx for 30 min, and the last dish was kept as a negative control. From all dishes, total cell extracts were obtained, the inputs were kept, and the rest of the cell lysates were incubated with anti-GFP antibody to immunoprecipitate hMAL-GFP; however, one of the extracts treated with Etx was incubated with anti- α -tubulin as a negative immunoprecipitation control. Western blot analysis performed after immunoprecipitation using anti-pEtx antibody revealed an Etx coimmunoprecipitate with hMAL-GFP (Fig. 4). It is remarkable that Etx was detected in the inputs and in coimmunoprecipitates as a large membrane complex. It is well-known that Etx oligomerizes and forms a large membrane complex, as previously described in the MDCK cell line (20). Etx was not detected when using the negative-control antibody (anti- α -tubulin). The same membrane was subsequently incubated with anti-GFP in order to check the correct immunoprecipitation of hMAL-GFP. Thus, the coimmunoprecipitation experiments indicated that Etx and MAL are able to interact.

The above-presented and previous results from other labs (22) suggest that MAL protein is required for the cytotoxic activity of Etx. If this is the case, those cells

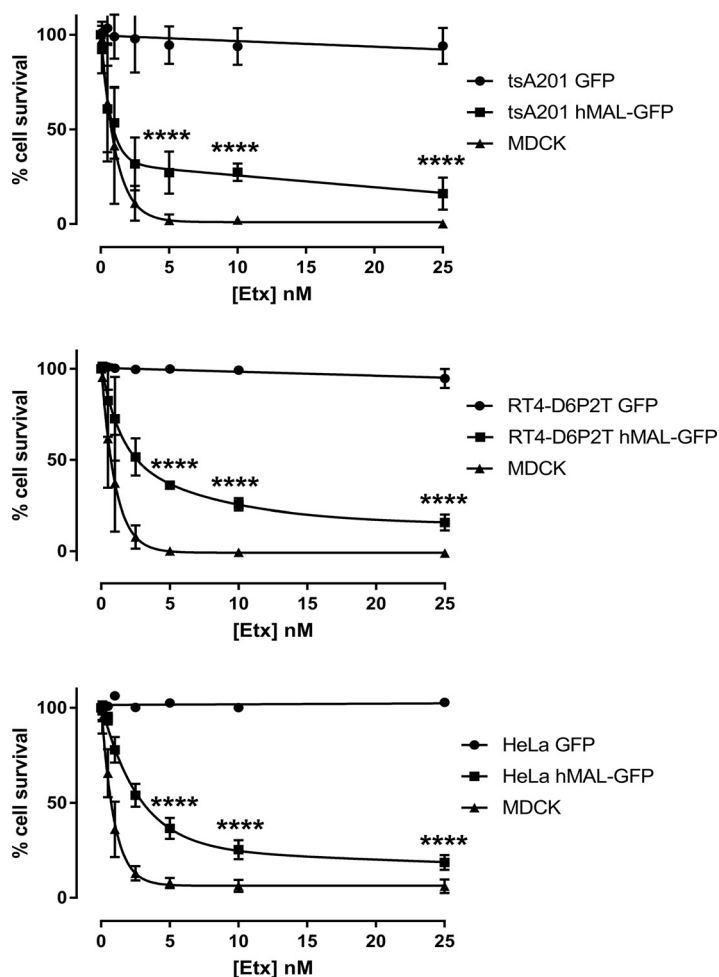


FIG 3 Cytotoxic effect of EtX on hMAL-GFP-expressing cells (tsA201, RT4-D6P2T, and HeLa cells). The MTS assay was performed to determine cell viability after incubating the cells with increasing concentrations of EtX for 1 h. Results from three independent experiments are represented as the percentage of cell survival at different EtX concentrations. The cytotoxicity of EtX on hMAL-GFP-expressing cells was dose dependent for MDCK cells, while no effect was observed for control cells expressing GFP alone. Each condition was run in triplicate and in three independent experiments (****, $P < 0.0001$; for clarity, only hMAL-GFP-expressing cells are labeled with asterisks).

expressing MAL protein could be potential targets of EtX. This suggestion is especially relevant for those cells of the immune system that may be involved directly or indirectly with neuroinflammatory and autoimmune diseases. To further study this possibility, we took advantage of cell lines of lymphocytic origin that express MAL protein and compared the results with those for cell lines of lymphocytic origin that do not express MAL protein.

MAL protein in lymphocytes. MAL protein was first identified in subsets of human lymphocyte populations, basically, T cell-derived cell lines, like the Jurkat and MOLT-4 human lymphocyte cell lines (24). Taking advantage of the natural expression of MAL protein in these cell lines, the possible effect of EtX was studied and compared with its effect in lymphocytic cell lines that do not express MAL protein (TK6 and JeKo-1, mantle-derived cell lines). The expression of MAL mRNA in MOLT-4 and Jurkat but not in TK6 and JeKo-1 cell lines was corroborated by reverse transcription-PCR (Fig. 5A). Notice that the assays with 18S rRNA, used as an internal control, indicated a constant expression level across all samples.

The effect of EtX on lymphocytic cell lines expressing MAL protein was confirmed by the MTS cytotoxicity assay (Fig. 5B), the ATP release assay (Fig. 5C), and flow cytometry

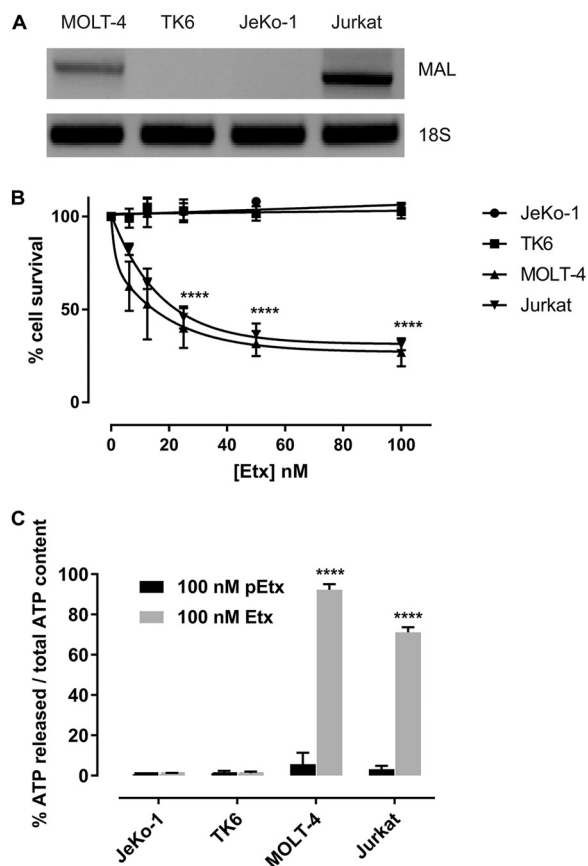


FIG 5 Lymphocytic cell lines expressing MAL are sensitive to Etx. (A) Reverse transcription-PCR detection of endogenous hMAL mRNA on MOLT-4 and Jurkat lymphocytic T cell lines but not on TK6 and JeKo-1 cell lines. The 18S rRNA was used as a control. (B) The MTS assay was performed as described in the legend to Fig. 3 to determine cell viability after treatment of cells (JeKo-1, TK6, MOLT-4, and Jurkat cells) with increasing concentrations of Etx for 1 h. The cytotoxicity of Etx on MOLT-4 and Jurkat cells was dose dependent, while no effect was observed on TK6 and JeKo-1 lymphocytic B cell lines. The results of triplicates of three independent experiments are represented as the percentage of cell survival at different Etx concentrations (****, $P < 0.0001$). (C) Percentage of ATP released from JeKo-1, TK6, MOLT-4, and Jurkat cells after treatment with 100 nM pEtx or Etx. MOLT-4 cells and Jurkat cells were sensitive to Etx, with ATP release being the highest in MOLT-4 cells, whereas no ATP release was observed in the JeKo-1 and TK6 lymphocytic B cell lines. Notice that no ATP release was detected when cells were incubated with pEtx at the maximum concentration of Etx used (100 nM). The histograms were obtained from triplicates of three independent experiments (****, $P < 0.0001$).

DISCUSSION

In this report, we show the direct interaction of epsilon toxin (Etx) from *Clostridium perfringens* with cells of the immune system. In humans, Etx has been involved with the onset of the neuroinflammatory and demyelinating disease multiple sclerosis (MS) (12). As far as we know, no relationship of Etx with the immune system has been described, and the possible involvement of this direct interaction with neuroinflammatory disease has not been described before.

Etx crosses the BBB and produces neurological alterations in sheep, goats, cattle, mice, and rats (31–33). Moreover, Etx induces glutamate release (5, 34) either by membrane pore formation (8) or through a membrane transporter (10), or through both systems, raising the intracellular receptor-mediated calcium concentration and producing a cytotoxic effect (5, 8, 10, 35). In fact, the lethal activity of Etx has been directly related to the neurological effect (31, 36).

It is assumed that the Etx-dependent ATP release is mediated by the pore formation of Etx after toxin oligomerization, which allows the efflux of molecules of up to ~2,300 Da from the cytosolic compartment (30). Similarly, Etx-dependent glutamate efflux

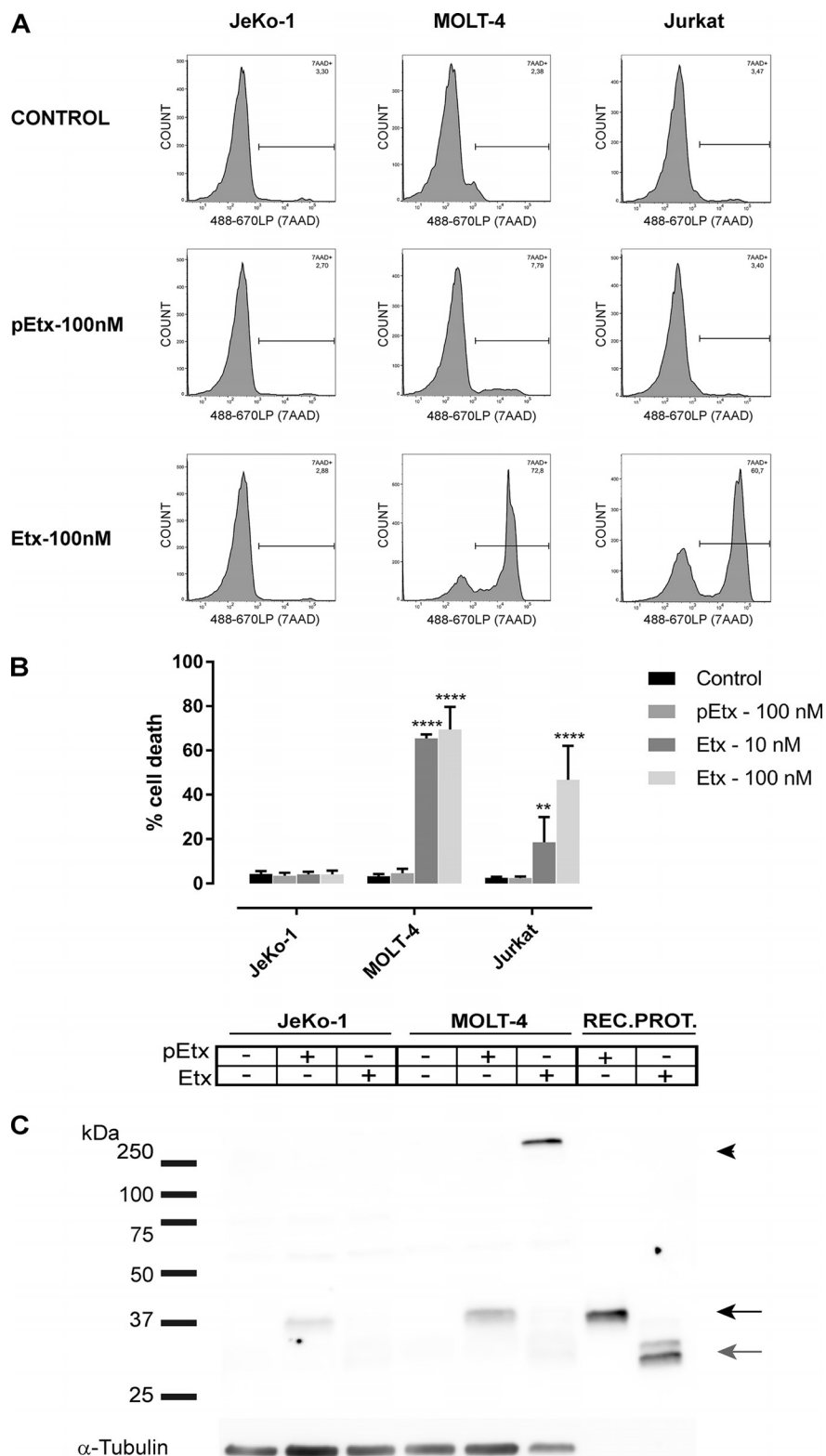


FIG 6 Etx cytotoxicity on MOLT-4 and Jurkat lymphocytic T cell lines is the result of oligomerization. (A) Flow cytometry and cell viability of JeKo-1, MOLT-4, and Jurkat cell lines after Etx incubation. Cells were incubated with 0, 10, and 100 nM pEtx or Etx for 20 min and analyzed after 7AAD staining. Histogram analysis of the 7AAD signal revealed that MOLT-4 and Jurkat cells were sensitive to Etx, while JeKo-1 cells were not sensitive at all. The bars indicate dead cells stained with 7AAD. 488-670LP, 488-nm excitation wavelength and 670LP detector/filter. Note that as in the case of JeKo-1, no cells died after pEtx incubation. The results are representative of those from one of three independent experiments. (B) Bar

(Continued on next page)

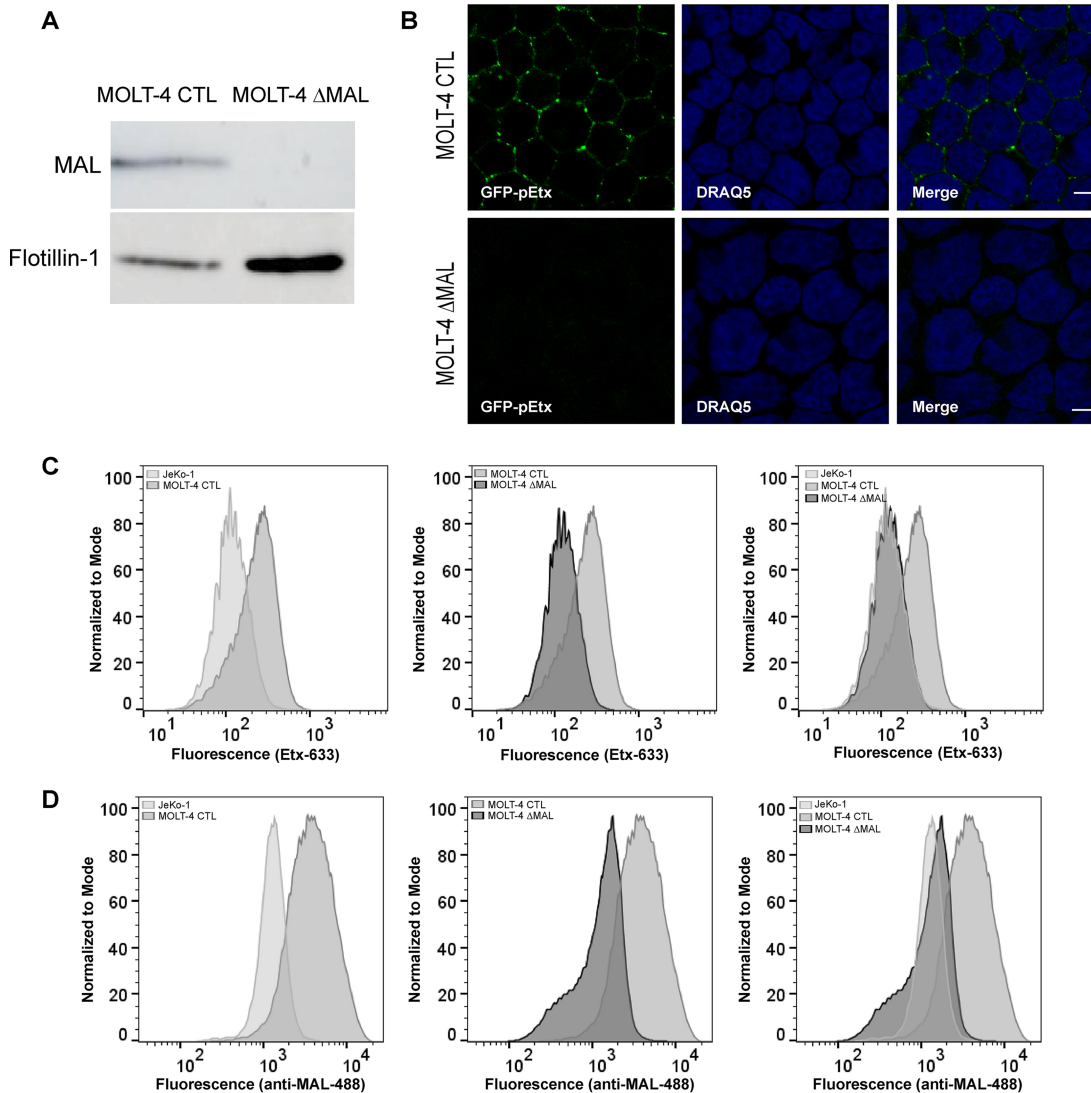


FIG 7 Etx binding depends on MAL expression. (A) Western blot analysis of MOLT-4 CTL and MOLT4 Δ MAL with anti-MAL-E1 antibody (top) and anti-flotillin-1 antibody (bottom) as a loading control. (Top) After applying the CRISPR-Cas9 technology, the MAL protein was absent on MOLT4 Δ MAL cells. The experiment was repeated three times. (B) Confocal microscopy images from MOLT-4 CTL and MOLT4 Δ MAL pelleted cells that had previously been incubated with 100 nM pEtx-GFP for 45 min. Nuclei were stained with DRAQ5 (blue). A high density of cells was observed after pelleted cells were resuspended in 20 μ l and placed as a drop on a coverslip. An intense fluorescent signal due to the pEtx binding was observed on the plasma membrane of MOLT-4 CTL cells (green) but not on MOLT4 Δ MAL cells. Bars, 5 μ m. (C) Flow cytometry analyses revealed the absence of Etx binding on MOLT-4 Δ MAL cells compared to MOLT-4 CTL cells after incubation of the cells with 100 nM Etx-633 for 20 min. (D) Flow cytometry analyses after incubation with anti-MAL 6D9 followed by Alexa Fluor 488-conjugated secondary antibody showed no anti-MAL 6D9 binding on MOLT-4 Δ MAL cells. Notice that MOLT-4 Δ MAL cells revealed no Etx binding or anti-MAL 6D9 binding due to the absence of MAL protein, as happened in JeKo-1 control cells.

from cells in the central nervous system (CNS) has been observed, although the rise in extracellular glutamate without a concomitant cytotoxic effect has also been ascribed to the glutamate membrane transporter (10). Accordingly, ATP could be at least partially extruded by a mechanism other than pore formation, including through

FIG 6 Legend (Continued)

chart of the cell death percentage determined by the flow cytometry assays explained above. Results were obtained from three independent experiments (**, $P = 0.0058$; ****, $P = 0.0001$). (C) JeKo-1 and MOLT-4 cell lines were treated with 100 nM pEtx or Etx for 30 min. Western blot analysis of cell lysates using anti-pEtx revealed high-molecular-weight complexes (>250 kDa, arrowhead) and monomeric forms of pEtx (black arrow) in MOLT-4 cells, but very low levels or no detection of pEtx or Etx was observed in the JeKo-1 cell line. Recombinant pEtx (black arrow) and Etx (gray arrow) were used as controls in the gels to define the correct-size bands, and the membrane was developed with anti- α -tubulin to obtain a loading control signal. The experiment was repeated three times.

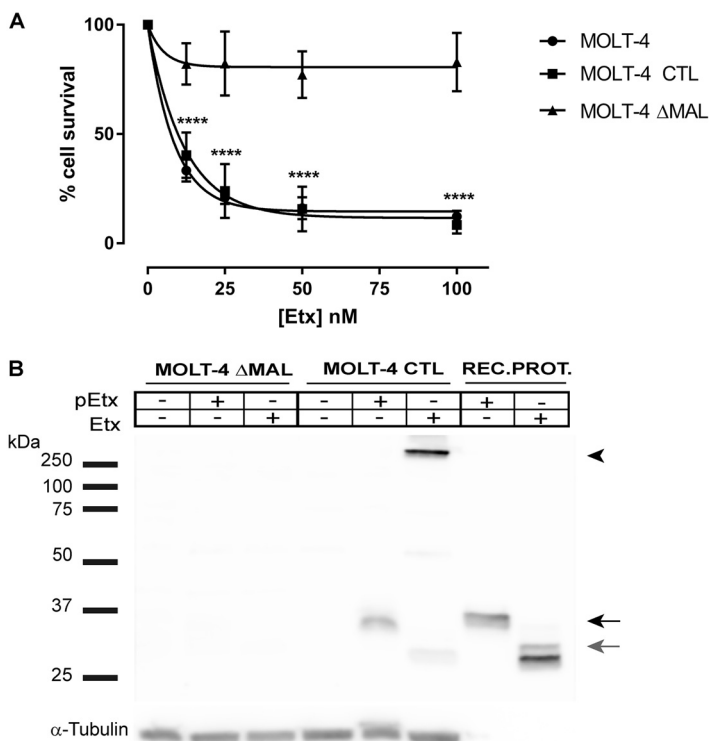


FIG 8 Neither cytotoxicity nor Etx binding and oligomeric complexes are detected on MOLT-4 ΔMAL cells. (A) The MTS assay was performed to determine cell viability after incubation of cells with increasing concentrations of Etx for 1 h. The cytotoxicity of Etx on MOLT-4 and MOLT-4 CTL cells was dose dependent, while no effect was observed on MOLT-4 ΔMAL cells. The results represent the percentage of cell survival from three independent experiments (****, $P < 0.0001$). (B) MOLT-4 CTL and MOLT-4 ΔMAL cells were treated with 100 nM pEtx or Etx for 30 min. Western blot analysis of cell lysates using anti-pEtx revealed oligomeric complexes (>250 kDa, arrowhead) and also monomeric forms of pEtx (black arrow) and Etx (gray arrow) in MOLT-4 CTL cells. No pEtx, Etx, or oligomeric complexes were observed in MOLT-4 ΔMAL cells. Recombinant pEtx and Etx were used as controls in the gels to define the correct-size bands, and the membrane was developed with anti-α-tubulin to obtain a loading control signal. The experiment was repeated three times.

membrane transporters or even by necrotic cell death, as has been shown for several pore-forming toxins (37). In any case, extracellular ATP may trigger the excitotoxicity of oligodendrocytes by the activation of P2X7 receptors, together with glutamate-mediated excitotoxicity (10, 38).

The present report supports a direct role of MAL protein in Etx activity (22). The expression of hMAL in the tsA201, RT4-D6P2T, and HeLa cell lines, which naturally do not express MAL protein, is sufficient to sensitize them to Etx, and, accordingly, cells naturally expressing MAL protein are sensitive to Etx. The effect of Etx on MAL protein-expressing cells was confirmed using up to three different methods: the MTS-based cell cytotoxicity assay and ATP release from transfected cell lines, together with the flow cytometry assay when lymphocyte-derived cell lines were used in the study. All three methods demonstrated the cytotoxic effect of Etx in the nanomolar range only on MAL-expressing cells, supporting the suggestion that this membrane protein is the cellular Etx receptor. Interestingly, MAL protein has been related to a defined membrane lipid composition, basically, in glycosphingolipid (mainly galactosylceramide and sulfatide)-enriched domains (39). Removal of the sulfate group significantly impairs Etx cytotoxic activity in MDCK cells, suggesting a close relationship between MAL protein, sulfatide, and Etx (19). Moreover, MAL protein has been involved in myelin biogenesis, probably in the vesicular transport of sulfatide to the membrane, forming myelin (39, 40).

Mice genetically deficient in MAL protein are resistant to Etx, suggesting that MAL

protein is involved not only in the cytotoxic effect of Etx on defined target cells but also in its lethal effect on naturally infected and experimental animal models.

As far as we know, this is the first time that a direct effect of Etx on a lymphocytic cell lineage, in particular, T cell-derived lymphocytes, has been shown. Moreover, the cytotoxic effect of Etx coincides with the expression of MAL protein in sensitive cell lines (24; this report) and is specific and dependent on MAL protein expression: deletion of MAL of protein expression in the MOLT-4 cell line completely abolished the cytotoxic effect of Etx.

What is the consequence of Etx acting on immune T cells? Although it is still speculative, it could represent the connection between Etx and its proposed role as an agent in the onset of MS. Different possibilities can be considered: (i) it may represent a situation where a direct but chronic exposure to low Etx concentrations and the property of Etx to bind both myelin and lymphocytes may induce an alteration in the myelin structure and in myelin formation or maintenance; (ii) Etx could have a direct effect on oligodendrocytes, producing their malfunction and even degeneration, with a consequent demyelination (10, 11) or a neuroinflammatory effect that would also cause alterations in myelin structures and subsequent demyelination; or (iii) Etx may directly act on a defined T cell population, either producing a cytotoxic effect or activating an immune response.

In the first possibility, the effect of Etx on lymphocytes would be time and concentration dependent. It could be assumed that circulating blood cells, in particular, a subpopulation of T cells wearing MAL protein, would be the first cell type in contact with Etx, together with endothelial cells, once in the bloodstream after toxin enters the organism even in very small amounts. Although the effect on immune cells could not be evident at such a low dose and no symptoms would be visible in a short time (which could be evident when a high number of T cells would be affected), T cells expressing MAL could be in contact with Etx for a long time, acting as Etx carriers and eventually entering the CNS, where they can interact with cells that, in turn, express MAL protein (oligodendrocytes). In the second possibility, as stated before, Etx binds to and eventually affects endothelial cells, crosses the BBB, and binds to myelin (9, 41), where it may act directly on oligodendrocytes, producing demyelination (10, 11). In the third possibility, Etx would act through a direct interaction with MAL protein-expressing T cells. In that case, Etx could activate a defined pool of T cells (those expressing MAL protein) and potentiate any of the above-proposed mechanisms in the onset of CNS demyelination or produce a cytotoxic effect on a regulatory T cell population, increasing the probability of an autoimmune reaction.

We understand that these suggestions are highly speculative, but they open a new view on the onset of neuroinflammatory diseases, where a particular gut microbiota component directly or indirectly interacts with the immune and nervous systems, affecting particular cell functions. While Etx may be the agent responsible for a demyelinating process, other components of the microbiota may influence or precipitate its onset (42). The animal model for MS, experimental autoimmune encephalomyelitis (EAE), is characterized by the contribution of CD4 T lymphocytes, especially Th1 and Th17 cells producing interferon gamma and interleukin 17, respectively (43, 44). It is widely accepted that MS, an autoimmune disease, is triggered by autoreactive T cells, which would be antigen activated, cross the BBB, and initiate an inflammatory response (45).

All together, these results show a direct interaction of Etx from *Clostridium perfringens* with T cells expressing MAL protein, suggesting a possible role in neuroinflammatory events and point out Etx (and pEtx) as a new marker for lymphocyte T cell lineages.

MATERIALS AND METHODS

Cell lines. Madin-Darby canine kidney (MDCK) cells (CCL-34; ATCC) were used as a positive control, as they are the most common sensitive *in vitro* model for Etx.

Three cell lines from different origins, tsA201 (catalog number 96121229; ECACC) from human kidney, RT4-D6P2T (CRL-2768; ATCC) from a rat schwannoma, and HeLa (a human epithelial cervix cell line from

an adenocarcinoma; CCL-2; ATCC), were selected because they do not express MAL protein and are insensitive to Etx.

Cell lines from different lymphocyte origins were chosen because of their capacity to express or not express MAL protein. TK6 (CRL-8015; ATCC), a human B lymphoblast cell line, and JeKo-1 (CRL-3006; ATCC), a mantle cell lymphoma cell line, do not express MAL protein. On the other hand, both Jurkat (catalog number 88042803; ECACC), a human leukemic T cell lymphoblast cell line, and MOLT-4 (catalog number 85011413; ECACC), a human acute T lymphoblastic leukemia cell line, express MAL protein.

The MDCK, tsA201, RT4-D6P2T, and HeLa cell lines were maintained in Dulbecco modified Eagle medium-F-12 medium containing 15 mM HEPES and 2.5 mM L-glutamine (Gibco) supplemented with 10% heat-inactivated fetal bovine serum (FBS; Biological Industries) and 1% penicillin-streptomycin (P-S; Sigma-Aldrich).

TK6, Jurkat, MOLT-4, and JeKo-1 cells were maintained in RPMI medium (Gibco) supplemented with 10% FBS (Biological Industries).

All cells were grown at 37°C in a humidified atmosphere of 5% CO₂. The cell lines, including the tsA201, RT4-D6P2T, and HeLa cell lines, were used to obtain stably transfected cells for the expression of pEGFPN1-hMAL or pEGFPN1 as a negative control. Cells were transfected using the Lipofectamine 2000 reagent (Invitrogen). After transfection, cells were selected with 0.5 mg/ml G418 (Geneticin; Gibco). Homogeneous GFP-expressing cells were obtained using a MoFlo Astrios cell sorter (Beckman Coulter) at CCITUB, Biology Unit of the Bellvitge Campus, University of Barcelona.

Expression of cDNA constructs of pEtx and GFP-pEtx. Expression vectors to produce a recombinant protein with a 6-histidine tag at the pEtx or GFP-pEtx C terminus were generated based on previously described plasmids (41). Plasmids were transformed into the *Escherichia coli* Rosetta(DE3)pLysS strain for optimum protein expression. The expression of pEtx or GFP-pEtx recombinant protein was induced overnight at room temperature in 250-ml LB medium cultures containing 1 mM isopropyl-β-D-thiogalactopyranoside. Cells were pelleted and resuspended in ice-cold phosphate buffer (PB; 0.02 M NaH₂PO₄/Na₂HPO₄, pH 7.4) containing 250 mM NaCl, sonicated, and centrifuged at 15,000 × *g* for 20 min at 4°C. The resulting supernatant was incubated with 0.5 ml of previously equilibrated Talon metal affinity resin that had previously been washed with PB and eluted with PB containing 250 mM imidazole. The eluate was dialyzed with phosphate-buffered saline (PBS; 0.01 M NaH₂PO₄/Na₂HPO₄, 150 mM NaCl, 2.7 mM KCl) at a final pH of 7.4 to eliminate imidazole, the final protein content was quantified, and the proteins were analyzed by SDS-PAGE and stored at -20°C until they were used. Full active toxin was obtained by trypsin proteolysis of pEtx or GFP-pEtx, using trypsin beads (Sigma-Aldrich) according to the manufacturer's instructions. The toxicities of pEtx and GFP-pEtx and their respective activated toxins were tested in MDCK cells as described elsewhere (14). The process of purification was performed following the guidelines of biosecurity of the University of Barcelona.

Cloning pEGFPN1-hMAL. The hMAL coding sequence (CDS) was obtained by PCR using 2 μl of a human cDNA brain library as the template, 25 μl KOD Hot Start DNA polymerase (Merck Millipore), and 1.5 μl oligonucleotides at 10 μM in a final 50-μl reaction volume. The oligonucleotides used were as follows: forward primer 5'-GCGAGATCTATGGCCCCGACGGCGACGGGGG-3' (containing a BglII target) and reverse primer 5'-GCGGTGACTGTGAAGACTTCCATCTGATTAAGAGAACACCGC-3' (containing a Sall target).

The reaction was carried out using the following parameters: 95°C for 2 min and 40 cycles of 95°C for 20 s, 60°C for 10 s, and 70°C for 10 s. The hMAL PCR product was purified using a QIAquick gel extraction kit (Qiagen). The purified PCR product was digested with the BglII-Sall restriction enzymes (Thermo Scientific), and the same enzymes were used to clone hMAL into pEGFPN1. Finally, the pEGFPN1-hMAL construct was sequenced to confirm the DNA sequence and to check the DNA insert orientation.

MAL protein detection by Western blot analysis. MAL protein expression in cell lines stably transfected with hMAL-GFP was detected by Western blot analysis. Confluent 10-cm-diameter culture plates were washed twice with phosphate-buffered saline (PBS). Cells were scraped with a cell scraper (catalog number 99002; TPP), the cell plate was maintained on ice, and 500 μl of radioimmunoprecipitation assay (RIPA) buffer (25 mM Tris-HCl, pH 7.4, 150 mM NaCl, 1% NP-40, 10% SDS, 1% sodium deoxycholate) supplemented with 1:100 protease inhibitor cocktail (catalog number P8340; Sigma-Aldrich) was added. Scraped cells were set into a 1.5-ml tube and incubated on ice for 30 min. The cells were disrupted by repeated aspiration through a 29-gauge (29G) needle and centrifuged at 20,000 × *g* for 15 min at 4°C. The pellet was discarded, and the supernatants, corresponding to total cell lysates, were quantified using a Pierce bicinchoninic acid (BCA) protein assay kit (Thermo Scientific). From total cell lysates, 30 μg was electrophoresed in a 10% polyacrylamide SDS-PAGE gel, transferred to a nitrocellulose membrane, and analyzed by Western blotting. A rabbit polyclonal anti-GFP tag (1:500 dilution; catalog number A-11122; Invitrogen) and mouse monoclonal anti-MAL-E1 (1:500 dilution; catalog number sc-390687; Santa Cruz), followed by secondary polyclonal swine anti-rabbit immunoglobulins-horseradish peroxidase (HRP) or polyclonal rabbit anti-mouse immunoglobulins-HRP, respectively (1:2,000 dilution; catalog number P0217 or P0161; Dako), were used.

The analysis of MAL endogenous protein expression in MOLT-4 cells was performed using a detergent-resistant membrane (DRM) enrichment protocol. Cells were lysed at 4°C in 200 μl of lysis buffer containing 1% Triton X-100, 0.5 mM EDTA, 1:100 protease inhibitor cocktail (catalog number P8340; Sigma-Aldrich). Lysates were passed through a 29G needle several times. The insoluble material (pellet I; nuclei, cytoskeleton, DRMs, and unbroken cells) was collected by centrifugation at 20,000 × *g* for 15 min at 4°C, and the supernatant was discarded. The sediment was resuspended in the lysis buffer supplemented with 60 mM octylglucoside, and the mixture was incubated at 37°C for 30 min to extract the DRMs. The resuspended pellet was centrifuged at 20,000 × *g* for 15 min at 4°C. The pellet was

discarded, and the supernatant with the extracted rafts containing MAL protein was collected. From total cell lysates, 30 μg was electrophoresed in a 12% polyacrylamide SDS-PAGE gel, transferred to a nitrocellulose membrane, and analyzed by Western blotting. The primary antibodies used were mouse monoclonal anti-MAL-E1 (1:500 dilution; catalog number sc-390687; Santa Cruz) and mouse monoclonal anti-flotillin-1 as a loading control (1:1,000 dilution; catalog number 610821; BD Bioscience). In both cases, incubation with the primary antibody was followed by incubation with secondary antibody consisting of polyclonal rabbit anti-mouse immunoglobulins-HRP (1:2,000 dilution; catalog number P0161; Dako).

The signal from the Western blotting membranes was developed with Luminata Crescendo Western HRP substrate (catalog number WBLUR0100; Merck) and detected using an Amersham Imager 600 (GE Healthcare Life Sciences).

EtX immunolocalization. tsA201, RT4-D6P2T, and HeLa transfected cells were grown to confluence on coverslips. The cells were washed three times with PBS and fixed with 4% paraformaldehyde (PFA) for 15 min at room temperature (RT). After 3 washings with PBS, cells were blocked by adding PBS containing 0.2% gelatin, 20% normal goat serum (NGS), and 0.05% Triton X-100 for 1 h at RT. Next, the cells were incubated with 200 nM EtX labeled with DyLight 633 (EtX-633) in PBS containing 0.2% gelatin, 1% NGS, 0.05% Triton X-100 for 1 h at RT. After three washes with PBS, coverslips were mounted with Fluoromount aqueous mounting medium (catalog number F4680; Sigma-Aldrich). EtX was labeled with DyLight 633 *N*-hydroxysuccinimide (NHS) ester (catalog number 46414; Thermo Scientific) following the manufacturer's instructions.

EtX immunolocalization on MOLT-4 CTL and MOLT-4 Δ MAL cells was performed starting from 2×10^6 cells. The cells were pelleted by centrifugation at $1,000 \times g$ for 3 min at 4°C, washed twice with 1 ml PBS, and fixed with 500 μl of 4% PFA at RT for 15 min. After fixation, the cells were pelleted by centrifugation at $1,000 \times g$ and washed three times with 1 ml PBS containing 1% bovine serum albumin (BSA) (PBS-1% BSA). A blocking step with buffer A (1 \times PBS, 0.2% gelatin, 20% normal goat serum [NGS], 3% BSA, 0.05% Triton X-100) was done at RT for 1 h, followed by an incubation at RT with 500 μl of 100 nM GFP-pEtX in buffer A for 45 min. After toxin incubation, the cells were stained with 500 μl of DRAQ5 (1:2,000 dilution; catalog number 108410; Abcam) in buffer A for 15 min at RT. Six washing steps were done by centrifugation at $1,000 \times g$ with 1 ml of PBS-1% BSA and 0.05% Triton X-100. Finally, the pellet was resuspended with 20 μl of Fluoromount aqueous mounting medium (catalog number F4680; Sigma-Aldrich) and placed on a coverslip.

Samples were analyzed by confocal microscopy in a Leica TCS-SL spectral confocal microscope at CCiTUB, Biology Unit of the Bellvitge Campus, University of Barcelona.

hMAL CRISPR-Cas9. hMAL small guide RNAs (sgRNAs) were designed using the sgRNA Scorer (version 2.0) CRISPR design tool (46). Several sgRNA sequences were obtained. Two hMAL sgRNAs were selected from the list; one matched the 5' untranslated region (UTR) and the other matched the CDS in a common sequence of hMAL mRNA variants.

The sequence of the hMAL-5'UTR sgRNA was CCCTGCTCTTAACCCGCGCGCGG, and that of the hMAL-CDS sgRNA was GCCCCGCAGCGCGCGGGGGG (underlined nucleotides correspond to protospacer adjacent motif [PAM] sequences and were not included in the design of oligonucleotides).

Oligonucleotides, including the selected sequences and overhangs for the step of ligation into the pair of BbsI restriction enzyme sites, were phosphorylated, annealed, and cloned into a pSPCas9(BB)-2A-GFP vector (Addgene plasmid 48138) as described by Ran et al. (47). Both hMAL sgRNA constructs, hMAL-5'UTRsgRNA-pSPCas9(BB)-2A-GFP and hMAL-CDSsgRNA-pSPCas9(BB)-2A-GFP, were cotransfected into MOLT-4 cells by electroporation to obtain MOLT-4 Δ MAL cells. In parallel, an empty pSPCas9(BB)-2A-GFP vector was also transfected into MOLT-4 cells to obtain a MOLT-4 CRISPR control cell line, MOLT-4 CTL. Cells were transfected by electroporation using a Gene Pulser apparatus with 4-mm-gap cuvettes (Bio-Rad) at 300 V and 10 ms with 1 pulse in an ECM 830 Electro Square Porator (BTX) electroporator.

After 24 h of transfection, a pool of GFP-positive cells was selected using a MoFlo Astrios cell sorter (Beckman Coulter) at CCiTUB, Biology Unit of the Bellvitge Campus, University of Barcelona. Afterwards, clonal selection from the GFP-positive pools was done using the same cell sorter. Clones were functionally checked by performing cytotoxicity assays.

Cytotoxicity assays. The cytotoxic effect of EtX was measured using the 3-(4,5-dimethylthiazol-2-yl)-5-(3-carboxymethoxyphenyl)-2-(4-sulfophenyl)-2H-tetrazolium (MTS) colorimetric assay. Cells were set into a 96-well cell culture plate at confluence (tsA201, RT4-D6P2T, and HeLa cells) or 80,000 cells/well for lymphoid cell lines in 100 μl RPMI medium (Gibco) supplemented with 10% FBS (Biological Industries). The cells were exposed to increasing concentrations of EtX (0, 6.25, 12.5, 25, 50, and 100 nM) for 1 to 2 h at 37°C. Controls were obtained by omitting EtX under each condition (100% cell viability) or by adding 0.1% Triton X-100 (100% cell lethality). After incubation, 20 μl CellTiter 96 AQ_{ueous} One cell proliferation reagent solution (catalog number G3581; Promega) was added to each well. The amount of formazan product obtained from the reaction was recorded spectrophotometrically at 490 nm in a microplate reader (Biochrom Asys UVM 340; Biochrom) at CCiTUB, Biology Unit of the Bellvitge Campus, University of Barcelona.

The absorbance obtained was directly proportional to the number of living cells in the culture. Triplicates of the assay were performed in three independent experiments for each condition. Statistics were determined by nonlinear regression analysis using a two-way analysis of variance (ANOVA) followed by Tukey's multiple-comparison test.

CT₅₀ values for cytotoxicity tests were determined from MTS assay absorbance values using a nonlinear regression model (curvefit) based on the sigmoidal dose-response curve (logarithm of inhibitor

versus normalized response). The CT_{50} with a 95% confidence interval (CI; lower-upper values) was calculated.

Luciferin-luciferase detection assay. Etx-dependent ATP release from cells was measured using the luciferin-luciferase method.

Adherent cells (tsA201, RT4-D6P2T, HeLa cells) were plated into a black 96-well plate with a clear flat bottom and grown to confluence in 100 μ l medium; in the case of suspension cells (JeKo-1, TK6, MOLT-4, and Jurkat cells), 80,000 cells/well were seeded in 100 μ l of medium.

The luciferase extract from the *Photinus pyralis* lantern (Sigma-Aldrich) was resuspended at 0.1 μ g/ μ l and desalted in a 10-ml 10 DG column (Bio-Rad). D-Luciferin (Sigma-Aldrich) was diluted at a concentration of 0.7 μ g/ μ l in ultrapure water and was adjusted with NaOH to a final pH of 7.4.

A mixture of 5 μ l of D-luciferin and 5 μ l of luciferase was added to each cell well. The light that was emitted when ATP reacted with the luciferin and luciferase was recorded in a FLUOstar Optima microplate reader (BMG) at CCIUB, Biology Unit of the Bellvitge Campus, University of Barcelona. Once the basal recording signal was stable, pEtx or Etx was added to each well to obtain the desired final concentration. When the peak bioluminescence returned to the basal level, Triton X-100 was added to evaluate the content of ATP still present in the cells. Each condition was run in triplicate in three independent experiments. Statistics were determined by nonlinear regression analysis using a two-way ANOVA, followed by Sidak's multiple-comparison test.

Oligomer complex formation. Etx cytotoxic activity is correlated with the formation of large membrane complexes (20). To observe the formation of Etx complexes in the plasma membrane, cells were grown and incubated with pEtx and Etx at 100 nM for 30 min at 37°C. The cells were pelleted by centrifugation at $800 \times g$, washed once with PBS, and centrifuged at $800 \times g$. The pellets were resuspended with 500 μ l of RIPA buffer supplemented with 1:100 protease inhibitor cocktail (catalog number P8340; Sigma-Aldrich), maintained on ice for 30 min, and homogenized by passage through a 29-gauge needle. The lysed cells were centrifuged at $20,000 \times g$ for 15 min. Supernatants, corresponding to total cell lysates, were quantified by use of a Pierce BCA protein assay kit (Thermo Scientific). Thirty micrograms of total cell lysates and 1 ng of recombinant pEtx and Etx, which were used as controls to detect the correct-size band, were electrophoresed in a 10% polyacrylamide SDS-PAGE gel and were transferred to nitrocellulose membranes. The membranes were analyzed by Western blotting using rabbit polyclonal anti-pEtx (14) preadsorbed to cell extracts (1:500 dilution), followed by polyclonal swine anti-rabbit immunoglobulins-HRP (1:15,000 dilution; catalog number P0217; Dako). The same membranes were developed with anti- α -tubulin clone DM 1A (1:2,000 dilution; catalog number T9026; Sigma-Aldrich) followed by rabbit anti-mouse immunoglobulins-HRP (1:15,000 dilution; catalog number P0161; Dako) to obtain the loading control. Membranes were developed with Luminata Crescendo Western HRP substrate (catalog number WBLUR0100; Merck), and the signal was detected using an Amersham Imager 600 (GE Healthcare Life Sciences).

Co-IP. The association of Etx and MAL was studied by coimmunoprecipitation (co-IP), which allows the study of protein-protein interactions. In the co-IP assays, the complexes containing the target protein were incubated with an antibody, and then Sepharose-protein A or -protein G beads were added to adsorb the antibody-protein complexes, which were obtained by centrifugation. The protein components in the complexes were visualized by Western blot analysis using specific antibodies raised against the different components.

HeLa cells expressing GFP (HeLa-pEGFPN1) and HeLa cells expressing hMAL-GFP (HeLa-pEGFPN1-hMAL) were grown to confluence in 10-cm-diameter cell culture dishes. Of the four HeLa-pEGFPN1-hMAL cell culture dishes, the cells in one dish were incubated for 30 min at 37°C with pEtx at 100 nM, the cells in two dishes were incubated with Etx at 100 nM, and the fourth dish was kept as a negative control. Cells were washed once with PBS, scraped, and resuspended with 500 μ l of RIPA buffer supplemented with protease inhibitor cocktail (catalog number P8340; Sigma-Aldrich). Cells were collected in a 1.5-ml tube and maintained on ice for 30 min. Suspensions were disrupted by repeated aspiration through a 29-gauge needle. The lysed cells were centrifuged at $20,000 \times g$ for 15 min, and the pellet was discarded. From the cell lysates, 20 μ l (4% total volume) for each condition was separated for use as input samples, and 10 μ l of 3 \times protein loading buffer (187.5 mM Tris-HCl, pH 6.8, 2% SDS, 0.006% bromophenol blue, 30% glycerol) containing 1% β -mercaptoethanol was added to each input.

A precleared lysate was obtained by adding 20 μ l of protein G plus/protein A-agarose suspension beads (catalog number IP-05; Merck) to the samples, which were incubated on a rotating device at 4°C for 1 h. The beads were pelleted by centrifugation at $1,000 \times g$ for 2 min at 4°C. The supernatants were transferred to a 1.5-ml tube, and 2 μ g of mouse monoclonal anti-GFP (clone GFP-20; catalog number G6539; Sigma-Aldrich) was added to all except one of the tubes, which had previously been incubated with 100 nM Etx and to which 2 μ g of mouse monoclonal anti- α -tubulin clone DM 1A (catalog number T9026; Sigma-Aldrich) was added as a negative control. The tubes were incubated overnight on a rotating device at 4°C. A volume of 30 μ l of protein G plus/protein A-agarose suspension beads was added to each tube, and the tubes were incubated at 4°C in a rotating device for 2 h. Immunoprecipitates adsorbed to beads were collected by centrifugation at $1,000 \times g$ for 2 min at 4°C. The supernatants were carefully aspirated and discarded. The pellets were washed 4 times with 1 ml RIPA buffer, and each time the above-described centrifugation step was repeated. After the final wash, the supernatants were aspirated and the resulting pellets were resuspended in 20 μ l protein loading buffer containing 1% β -mercaptoethanol. All samples were heated for 5 min at 95°C and centrifuged at $1,000 \times g$ for 2 min at 4°C to separate the agarose beads. The inputs, supernatants, and recombinant proteins pEtx and Etx were loaded in a 10% polyacrylamide SDS-PAGE gel, transferred to a nitrocellulose membrane, and detected by Western blot analysis with anti-pEtx rabbit polyclonal antibody preadsorbed to cell extracts

(1:500 dilution) (14), followed by secondary polyclonal swine anti-rabbit immunoglobulins HRP (1:15,000 dilution; catalog number P0217; Dako), to reveal the coimmunoprecipitated MAL-GFP protein and Etx.

Afterwards, the same membrane was reblotted to check the immunoprecipitated MAL protein-GFP with mouse monoclonal anti-GFP clone GFP-20 (1:500 dilution; catalog number G6539; Sigma-Aldrich) followed by secondary polyclonal rabbit anti-mouse immunoglobulins HRP (1:15,000 dilution; catalog number P0161; Dako).

The signal from the membranes was developed with Luminata Crescendo Western HRP substrate (catalog number WBLUR0100; Merck) and detected using an Amersham Imager 600 (GE Healthcare Life Sciences).

Reverse transcription-PCR. Total RNA extraction from TK6, JeKo-1, MOLT-4, and Jurkat-1 cells was realized using an RNeasy minikit (Qiagen) following the manufacturer's instructions.

The concentration of each sample was recorded spectrophotometrically at 260 nm in a NanoDrop 2000C spectrophotometer (Thermo Scientific). A retrotranscription reaction (1.5 μ g RNA) was carried out by using a RevertAid first-strand cDNA synthesis kit (Thermo Scientific) following the protocol provided by the supplier. PCRs were performed using 2 \times PCR master mix (Thermo Scientific) to detect the presence of hMAL cDNA or 18S rRNA.

The hMAL primers were hMAL Forward (5'-GCGAAGCTTATGGCCCCGAGCGGCGACGGGGG-3') and hMAL Reverse (5'-GCGCTCGAGTGAAGACTTCCATCTGATTAAGAGAACCACCGC-3'). The 18S rRNA primers were 18S Forward (5'-CGCAGAATCCCACTCCCGACCC-3') and 18S Reverse (5'-CCCAAGTCCAACTACGAGC-3').

The reactions were carried out using the following parameters: 95°C for 2 min and 40 cycles of 95°C for 20 s, 62°C for 10 s, and 70°C for 10 s. Amplicons were detected by electrophoresis in a 2% agarose gel.

Flow cytometry. The flow cytometry experiments to analyze the sensitivity of the cells to Etx were performed starting with 6×10^6 cells/tube. The cells were incubated with 100 nM Etx-633 in RPMI medium supplemented with 10% FBS for 20 min. The cells were centrifuged at $1,500 \times g$ for 5 min at 4°C and washed twice with 1 ml PBS-1% BSA. Finally, 5 μ l of 7-aminoactinomycin (7AAD; Invitrogen) was added before flow cytometry analysis. Triplicates of the assay were performed in three independent experiments, and statistics were determined by nonlinear regression analysis using a two-way ANOVA followed by Dunnett's multiple-comparison test.

To check the binding of Etx to different cell lines, cells were incubated for 20 min with 100 nM Etx-633 in RPMI medium supplemented with 10% FBS and 3% BSA, centrifuged at $1,500 \times g$ for 5 min at 4°C, and washed twice with 1 ml PBS-1% BSA. The cells were fixed with 4% PFA for 15 min at RT. After fixation, the cells were pelleted by centrifugation at $1,500 \times g$ and washed three times with 1 ml of PBS-1% BSA. A blocking step with buffer A (1 \times PBS, 0.2% gelatin, 20% normal goat serum [NGS], 3% BSA, 0.05% Triton X-100) was done for 30 min at RT, followed by an incubation with mouse monoclonal anti-MAL 6D9 antibody (1:300 dilution) (48) for 30 min at RT in 500 μ l of buffer A. After three washes, the cells were centrifuged at $1,500 \times g$, and the pellet was resuspended with PBS-1% BSA. Secondary antibody incubation was performed with goat anti-mouse immunoglobulin-Alexa Fluor 488 (1:2,000 dilution; catalog number A11029; Invitrogen) in buffer A. Finally, the cells were washed three times with PBS-1% BSA. Samples were analyzed in a BD FACSCanto flow cytometer (BD Biosciences, San Diego, CA) at CCITUB, Biology Unit of the Bellvitge Campus, University of Barcelona, and the data were analyzed using FlowJo software (FlowJo LLC, Ashland, OR).

Quantification and statistical analysis. Statistical parameters, including assays, *n* values, comparison tests, and statistical significance, are reported in the specific Materials and Methods section, figures, and figure legends. In the figures, asterisks denote statistical significance, calculated by nonlinear regression analysis using a two-way ANOVA, and each *P* value is indicated in the figure legends.

All statistics were analyzed using Prism (version 7.00) software for Windows (GraphPad Software, La Jolla, CA).

ACKNOWLEDGMENTS

We thank Miguel Angel Alonso from the Centro de Biología Molecular Severo Ochoa (CSIC-UAM, Spain) for the anti-MAL 6D9 antibody and useful comments, Joan Gil from the Department of Physiological Sciences of the University of Barcelona for the TK6, Jurkat, and JeKo-1 cell lines, and Mireia Martin from the Pathology and Experimental Therapeutics Department of the University of Barcelona for the 18S rRNA primers.

This work was supported by grants SAF2014-56811-R and SAF2017-85818-R from the Ministerio de Economía, Industria y Competitividad, la Agencia Estatal de Investigación, and cofunded by FEDER funds/European Regional Development Fund (ERDF)-a Way To Build Europe, to J.B. and C.S.

REFERENCES

- Payne D, Oyston P. 1997. The *Clostridium perfringens* epsilon toxin. Academic Press, San Diego, CA.
- Songer JG. 1996. Clostridial enteric diseases of domestic animals. Clin Microbiol Rev 9:216-234.
- Uzal FA, Songer JG. 2008. Diagnosis of *Clostridium perfringens* intestinal infections in sheep and goats. J Vet Diagn Invest 20:253-265. <https://doi.org/10.1177/104063870802000301>.
- Minami J, Katayama S, Matsushita O, Matsushita C, Okabe A. 1997. Lambda-toxin of *Clostridium perfringens* activates the precursor of epsilon-toxin by releasing its N- and C-terminal peptides. Microbiol

- Immunol 41:527–535. <https://doi.org/10.1111/j.1348-0421.1997.tb01888.x>.
5. Miyamoto O, Minami J, Toyoshima T, Nakamura T, Masada T, Nagao S, Negi T, Itano T, Okabe A. 1998. Neurotoxicity of *Clostridium perfringens* epsilon-toxin for the rat hippocampus via the glutamatergic system. *Infect Immun* 66:2501–2508.
 6. Cole AR, Gibert M, Popoff M, Moss DS, Titball RW, Basak AK. 2004. *Clostridium perfringens* epsilon-toxin shows structural similarity to the pore-forming toxin aerolysin. *Nat Struct Mol Biol* 11:797–798. <https://doi.org/10.1038/nsmb804>.
 7. Popoff MR. 2014. Clostridial pore-forming toxins: powerful virulence factors. *Anaerobe* 30:220–238. <https://doi.org/10.1016/j.anaerobe.2014.05.014>.
 8. Popoff M. 2011. Epsilon toxin: a fascinating pore-forming toxin. *FEBS J* 278:4602–4615. <https://doi.org/10.1111/j.1742-4658.2011.08145.x>.
 9. Dorca-Arevalo J, Soler-Jover A, Gibert M, Popoff M, Martin-Satue M, Blasi J. 2008. Binding of epsilon-toxin from *Clostridium perfringens* in the nervous system. *Vet Microbiol* 131:14–25. <https://doi.org/10.1016/j.vetmic.2008.02.015>.
 10. Wioland L, Dupont J, Doussau F, Gaillard S, Heid F, Isope P, Pauillac S, Popoff M, Bossu J, Poulain B. 2015. Epsilon toxin from *Clostridium perfringens* acts on oligodendrocytes without forming pores, and causes demyelination. *Cell Microbiol* 17:369–388. <https://doi.org/10.1111/cmi.12373>.
 11. Linden J, Ma Y, Zhao B, Harris J, Rumah K, Schaeren-Wiemers N, Vartanian T. 2015. *Clostridium perfringens* epsilon toxin causes selective death of mature oligodendrocytes and central nervous system demyelination. *mBio* 6:e02513-14. <https://doi.org/10.1128/mBio.02513-14>.
 12. Rumah KR, Linden J, Fischetti VA, Vartanian T. 2013. Isolation of *Clostridium perfringens* type B in an individual at first clinical presentation of multiple sclerosis provides clues for environmental triggers of the disease. *PLoS One* 8:e76359. <https://doi.org/10.1371/journal.pone.0076359>.
 13. Tamai E, Ishida T, Miyata S, Matsushita O, Suda H, Kobayashi S, Sonobe H, Okabe A. 2003. Accumulation of *Clostridium perfringens* epsilon-toxin in the mouse kidney and its possible biological significance. *Infect Immun* 71:5371–5375. <https://doi.org/10.1128/IAI.71.9.5371-5375.2003>.
 14. Soler-Jover A, Blasi J, Gómez de Aranda I, Navarro P, Gibert M, Popoff MR, Martín-Satué M. 2004. Effect of epsilon toxin-GFP on MDCK cells and renal tubules in vivo. *J Histochem Cytochem* 52:931–942. <https://doi.org/10.1369/jhc.4A6254.2004>.
 15. Chassin C, Bens M, de Barry J, Courjaret R, Bossu JL, Cluzeaud F, Ben Mkaddem S, Gibert M, Poulain B, Popoff MR, Vandewalle A. 2007. Pore-forming epsilon toxin causes membrane permeabilization and rapid ATP depletion-mediated cell death in renal collecting duct cells. *Am J Physiol Renal Physiol* 293:F927–F937. <https://doi.org/10.1152/ajprenal.00199.2007>.
 16. Shortt SJ, Titball RW, Lindsay CD. 2000. An assessment of the in vitro toxicology of *Clostridium perfringens* type D epsilon-toxin in human and animal cells. *Hum Exp Toxicol* 19:108–116. <https://doi.org/10.1191/096032700678815710>.
 17. Fernandez Miyakawa ME, Zabal O, Silberstein C. 2011. *Clostridium perfringens* epsilon toxin is cytotoxic for human renal tubular epithelial cells. *Hum Exp Toxicol* 30:275–282. <https://doi.org/10.1177/0960327110371700>.
 18. Ivie SE, Fennessey CM, Sheng J, Rubin DH, McClain MS. 2011. Gene-trap mutagenesis identifies mammalian genes contributing to intoxication by *Clostridium perfringens* epsilon-toxin. *PLoS One* 6:e17787. <https://doi.org/10.1371/journal.pone.0017787>.
 19. Gil C, Dorca-Arevalo J, Blasi J. 2015. *Clostridium perfringens* epsilon toxin binds to membrane lipids and its cytotoxic action depends on sulfatide. *PLoS One* 10:e0140321. <https://doi.org/10.1371/journal.pone.0140321>.
 20. Petit L, Gibert M, Gillet D, Laurent-Winter C, Boquet P, Popoff MR. 1997. *Clostridium perfringens* epsilon-toxin acts on MDCK cells by forming a large membrane complex. *J Bacteriol* 179:6480–6487. <https://doi.org/10.1128/jb.179.20.6480-6487.1997>.
 21. Nagahama M, Hara H, Fernandez-Miyakawa M, Itohayashi Y, Sakurai J. 2006. Oligomerization of *Clostridium perfringens* epsilon-toxin is dependent upon membrane fluidity in liposomes. *Biochemistry* 45:296–302. <https://doi.org/10.1021/bi051805s>.
 22. Rumah K, Ma Y, Linden J, Oo M, Anrather J, Schaeren-Wiemers N, Alonso M, Fischetti V, McClain M, Vartanian T. 2015. The myelin and lymphocyte protein MAL is required for binding and activity of *Clostridium perfringens* epsilon-toxin. *PLoS Pathog* 11:e1004896. <https://doi.org/10.1371/journal.ppat.1004896>.
 23. Khalili S, Jahangiri A, Hashemi Z, Khalesi B, Mard-Soltani M, Amani J. 2017. Structural pierce into molecular mechanism underlying *Clostridium perfringens* epsilon toxin function. *Toxicon* 127:90–99. <https://doi.org/10.1016/j.toxicon.2017.01.010>.
 24. Alonso M, Weissman S. 1987. cDNA cloning and sequence of MAL, a hydrophobic protein associated with human T-cell differentiation. *Proc Natl Acad Sci U S A* 84:1997–2001.
 25. Cheong K, Zacchetti D, Schneeberger E, Simons K. 1999. VIP17/MAL, a lipid raft-associated protein, is involved in apical transport in MDCK cells. *Proc Natl Acad Sci U S A* 96:6241–6248.
 26. Marazuela M, Alonso M. 2004. Expression of MAL and MAL2, two elements of the protein machinery for raft-mediated transport, in normal and neoplastic human tissue. *Histol Histopathol* 19:925–933. <https://doi.org/10.14670/HH-19.925>.
 27. Alonso M, Millan J. 2001. The role of lipid rafts in signalling and membrane trafficking in T lymphocytes. *J Cell Sci* 114:3957–3965.
 28. Ventimiglia L, Fernandez-Martin L, Martinez-Alonso E, Anton O, Guerra M, Martin-Menarguez J, Andres G, Alonso M. 2015. Cutting edge: regulation of exosome secretion by the integral MAL protein in T cells. *J Immunol* 195:810–814. <https://doi.org/10.4049/jimmunol.1500891>.
 29. Petit L, Maier E, Gibert M, Popoff MR, Benz R. 2001. *Clostridium perfringens* epsilon toxin induces a rapid change of cell membrane permeability to ions and forms channels in artificial lipid bilayers. *J Biol Chem* 276:15736–15740. <https://doi.org/10.1074/jbc.M010412200>.
 30. Nestorovich E, Karginov V, Bezrukov S. 2010. Polymer partitioning and ion selectivity suggest asymmetrical shape for the membrane pore formed by epsilon toxin. *Biophys J* 99:782–789. <https://doi.org/10.1016/j.bpj.2010.05.014>.
 31. Finnie JW. 2004. Neurological disorders produced by *Clostridium perfringens* type D epsilon toxin. *Anaerobe* 10:145–150. <https://doi.org/10.1016/j.anaerobe.2003.08.003>.
 32. Uzal F, Kelly W, Morris W, Assis R. 2002. Effects of intravenous injection of *Clostridium perfringens* type D epsilon toxin in calves. *J Comp Pathol* 126:71–75. <https://doi.org/10.1053/jcpa.2001.0514>.
 33. Finnie JW, Blumbergs PC, Manavis J. 1999. Neuronal damage produced in rat brains by *Clostridium perfringens* type D epsilon toxin. *J Comp Pathol* 120:415–420. <https://doi.org/10.1053/jcpa.1998.0289>.
 34. Miyamoto O, Sumitani K, Nakamura T, Yamagami S, Miyata S, Itano T, Negi T, Okabe A. 2000. *Clostridium perfringens* epsilon toxin causes excessive release of glutamate in the mouse hippocampus. *FEMS Microbiol Lett* 189:109–113. <https://doi.org/10.1111/j.1574-6968.2000.tb09215.x>.
 35. Lonchamp E, Dupont JL, Wioland L, Courjaret R, Mbebi-Liegeois C, Jover E, Doussau F, Popoff MR, Bossu JL, de Barry J, Poulain B. 2010. *Clostridium perfringens* epsilon toxin targets granule cells in the mouse cerebellum and stimulates glutamate release. *PLoS One* 5:e13046. <https://doi.org/10.1371/journal.pone.0013046>.
 36. Uzal F, Vidal J, McClane B, Gurjar A. 2010. *Clostridium perfringens* toxins involved in mammalian veterinary diseases. *Open Toxicology J* 2:24–42. <https://doi.org/10.2174/1875414701003020024>.
 37. Bischofberger M, Iacovache I, van der Goot F. 2012. Pathogenic pore-forming proteins: function and host response. *Cell Host Microbe* 12:266–275. <https://doi.org/10.1016/j.chom.2012.08.005>.
 38. Matute C. 2011. Glutamate and ATP signalling in white matter pathology. *J Anat* 219:53–64. <https://doi.org/10.1111/j.1469-7580.2010.01339.x>.
 39. Frank M. 2000. MAL, a proteolipid in glycosphingolipid enriched domains: functional implications in myelin and beyond. *Prog Neurobiol* 60:531–544. [https://doi.org/10.1016/S0301-0082\(99\)00039-8](https://doi.org/10.1016/S0301-0082(99)00039-8).
 40. Kim T, Fiedler K, Madison D, Krueger W, Pfeiffer S. 1995. Cloning and characterization of MVP17. A developmentally regulated myelin protein in oligodendrocytes. *J Neurosci Res* 42:413–422.
 41. Soler-Jover A, Dorca J, Popoff MR, Gibert M, Saura J, Tusell JM, Serratos J, Blasi J, Martín-Satué M. 2007. Distribution of *Clostridium perfringens* epsilon toxin in the brains of acutely intoxicated mice and its effect upon glial cells. *Toxicon* 50:530–540. <https://doi.org/10.1016/j.toxicon.2007.04.025>.
 42. Berer K, Gerdes L, Cekanaviciute E, Jia X, Xiao L, Xia Z, Liu C, Klotz L, Stauffer U, Baranzini S, Kumpfel T, Hohlfeld R, Krishnamoorthy G, Wekerle H. 2017. Gut microbiota from multiple sclerosis patients enables spontaneous autoimmune encephalomyelitis in mice. *Proc Natl Acad Sci U S A* 114:10719–10724. <https://doi.org/10.1073/pnas.1711233114>.
 43. Constantinescu C, Farooqi N, O'Brien K, Gran B. 2011. Experimental

- autoimmune encephalomyelitis (EAE) as a model for multiple sclerosis (MS). *Br J Pharmacol* 164:1079–1106. <https://doi.org/10.1111/j.1476-5381.2011.01302.x>.
44. Sonar S, Lal G. 2017. Differentiation and transmigration of CD4 T cells in neuroinflammation and autoimmunity. *Front Immunol* 8:1695. <https://doi.org/10.3389/fimmu.2017.01695>.
45. Lindner M, Klotz L, Wiendl H. 25 March 2018. Mechanisms underlying lesion development and lesion distribution in CNS autoimmunity. *J Neurochem*. <https://doi.org/10.1111/jnc.14339>.
46. Chari R, Yeo N, Chavez A, Church G. 2017. sgRNA Scorer 2.0: a species-independent model to predict CRISPR/Cas9 activity. *ACS Synth Biol* 6:902–904. <https://doi.org/10.1021/acssynbio.6b00343>.
47. Ran F, Hsu P, Wright J, Agarwala V, Scott D, Zhang F. 2013. Genome engineering using the CRISPR-Cas9 system. *Nat Protoc* 8:2281–2308. <https://doi.org/10.1038/nprot.2013.143>.
48. Martin-Belmonte F, Kremer L, Albar J, Marazuela M, Alonso M. 1998. Expression of the MAL gene in the thyroid: the MAL proteolipid, a component of glycolipid-enriched membranes, is apically distributed in thyroid follicles. *Endocrinology* 139:2077–2084. <https://doi.org/10.1210/endo.139.4.5875>.